Femtosecond Yb:YAG laser using semiconductor saturable absorbers

C. Hönninger, G. Zhang, and U. Keller

Ultrafast Laser Physics, Institute of Quantum Electronics, Swiss Federal Institute of Technology, ETH Hönggerberg–HPT, CH-8093 Zürich, Switzerland

A. Giesen

Institut für Strahlwerkzeuge, Universität Stuttgart, Pfaffenwaldring 43, D-70569 Stuttgart, Germany

Received July 31, 1995

We demonstrate a passively mode-locked femtosecond Yb:YAG laser using different semiconductor saturable absorber devices, a high-finesse and a low-finesse antiresonant Fabry–Perot saturable absorber. We achieved pulses as short as 540 fs with dispersion compensation and 1.7-ps pulses without dispersion compensation. We also mode locked the laser at either 1.03 or 1.05 μm by adjusting the band gap and antiresonance wavelength design of the antiresonant Fabry–Perot saturable absorber. © 1995 Optical Society of America

Yb:YAG is interesting as a high-power diode-pumped laser source because of its low thermal loading and its wide absorption band at 940 nm.[1,2] A power-scalable concept that uses these features was recently demonstrated.[3] Additionally, Yb:YAG has a broad emission spectrum, supporting tunability[4,5] and femtosecond pulse generation in the few-hundred-femtosecond regime. We previously demonstrated simple, femtosecond passive mode locking of diode-pumped Nd:glass,[6] Cr:LiSAF,[7,8] and argon-ion-pumped Ti:sapphire[9,10] lasers that used an antiresonant Fabry–Perot saturable absorber[11,12] (A-FPSA) and generated pulses as short as 19 fs.[10] Power scalability of the A-FPSA is also feasible by adjustment of both the incident laser spot size on the absorber and the top reflectivity with respect to the intracavity power.[13] For high-power applications thermal problems in the A-FPSA device could be addressed by face cooling similar to the thin disk concept.[3] Therefore an A-FPSA mode-locked Yb:YAG laser is a potentially promising approach to obtaining high peak powers with high average power.

We demonstrate a passively mode-locked Yb:YAG laser generating stable and self-starting pulses as short as 540 fs with typical average output powers of 150 mW. Previously, only active mode locking in Yb:YAG had been demonstrated, with a pulse duration of 80 ps.[14] We achieved mode locking at either 1.03 or 1.05 μm, depending on the design of the band gap and the antiresonance wavelength of the A-FPSA. Without dispersion compensation in the laser we obtained pulses as short as 1.7 ps. Additionally, using both a high-finesse and a low-finesse A-FPSA, we demonstrate power scaling with the top reflector and absorber thickness as the adjustable parameters.

Figure 1 shows the designs of the two devices. The high-finesse A-FPSA is shown in Fig. 1(a) and described in Ref. 13. The low-finesse A-FPSA[9,10,15] [Fig. 1(b)] takes into account standing-wave effects. The InGaAs absorber layer is placed between transparent layers. GaAs was used on top to reduce oxidation effects. The low-finesse A-FPSA structure is formed because the absorber is placed between a high-reflecting bottom mirror and a top reflector of $\approx 30\%$ that is due to the Fresnel reflection at the air–GaAs interface. The low-finesse A-FPSA requires a higher reflectivity of the bottom reflector [25 pairs of AlAs/GaAs layers instead of only 16 pairs as in Fig. 1(a)] to reduce its cavity insertion loss to an acceptable level.[10] Both saturable absorbers provide the same maximum modulation depth of $\approx 0.5\%$; however, the saturation fluence E_{sat} is 4.5 mJ/cm^2 for the high-finesse A-FPSA and 120 μJ/cm^2 (i.e., 40 times smaller) for the low-finesse A-FPSA. The saturation fluence of the high-finesse A-FPSA was measured with 1.4-ps pulses.[13] For the low-finesse A-FPSA we estimate the saturation fluence by taking into account the lower top reflector and the fact that the absorbing layer is matched to the peak of the standing wave inside the A-FPSA by appropriate spacer layers [Fig. 1(b)]. Both saturable absorbers exhibit a bitemporal impulse response with a fast component of $\approx$200 fs and a slow component (i.e., the carrier lifetime) τ_c of 3.8 ps for the high-finesse and 6 ps for the low-finesse A-FPSA.[13]

Yb:YAG has a long upper-state lifetime of $\approx$1 ms, which strongly increases its tendency for self-Q-switched mode locking.[16] Thus both the saturation intensity I_{sat} and the saturation fluence E_{sat} of the saturable absorber need to be carefully adapted to the available operation power for stable self-starting mode locking. The main adjustable parameters of the A-FPSA are the incident mode size, the top reflector, and the impulse response.[13] Both the incident mode area and the top reflector adjust I_{sat} and E_{sat} equally because $I_{\mathrm{sat}} \cong E_{\mathrm{sat}}/\tau_c$ for pulse durations shorter than τ_c, which is typically the case for our saturable absorbers. However, the carrier lifetime is a design parameter that affects only I_{sat}. For semiconductor saturable absorbers the carrier lifetime can be set with the molecular-beam epitaxy (MBE) growth

0146-9592/95/232402-03$6.00/0

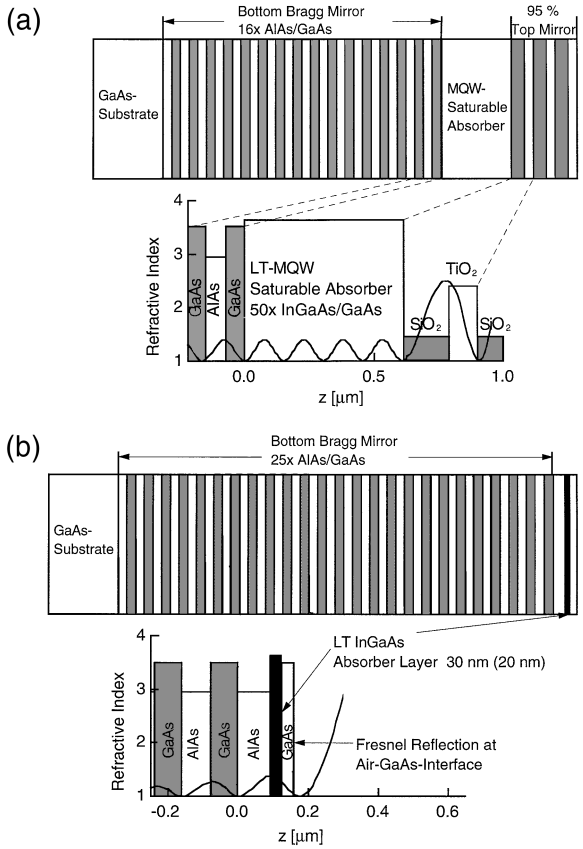

Fig. 1. Schematic structure of the semiconductor saturable absorbers: (a) high-finesse A-FPSA and (b) low-finesse A-FPSA designed for 1.05 μm. The low-finesse design for 1.03 μm used a thinner absorber layer (20 nm) and a thinner spacer layer to increase the nonsaturable loss at 1.05 μm. LT, low-temperature MBE growth; MQW, multiple quantum well.

temperature from nanoseconds to subpicoseconds (i.e., 4 orders of magnitude). Therefore the top reflector and the mode size are used to adjust E_{sat} to the available intracavity pulse energy. Maximum modulation depth and therefore shorter pulses are obtained for pulse energy densities that are a few times the saturation fluence. It is also important to note that a lower top reflector also requires a thinner absorber layer to reduce the insertion loss [Fig. 1(b)]. The saturation intensity has to be large enough to prevent self-Q switching but small enough to provide self-starting mode locking.[16] Reducing the carrier lifetime in semiconductor saturable absorbers to the 10 ps-regime with low-temperature MBE growth sufficiently increased I_{sat} with only small degradation of the modulation depth and without too many residual nonsaturable losses.[13] This adjustability led to the first stable intracavity passive mode locking of solid-state lasers, such as Nd:YAG and Nd:YLF,[11] with long upper-state lifetimes.

Figure 2 is a schematic of the laser setup with and without dispersion compensation. The Yb:YAG crystal thickness d is approximately twice the absorption length ($d = 3.5$ mm, 5% Yb doping). Both sides of the crystal are pumped to minimize reabsorption losses at the laser wavelength in this quasi-three-level system. The 940-nm pump light of the Ti:sapphire laser is focused to a 27-μm spot radius inside the crystal with a confocal parameter of 2.4 mm. In all measurements we used a 2% output coupler.

To passively mode lock the laser we substitute a curved mirror for one flat end mirror of the delta cavity to focus onto the absorber (Fig. 2). With an available pump power of $\sim$1.5 W we reach typical intracavity powers of 5–10 W. We then use a 7.5-cm radius-of-curvature (ROC) focusing mirror with the high-finesse and a 40-cm ROC mirror with the low-finesse A-FPSA. This results in focused beam radii of 12 and 80 μm on the semiconductor devices and therefore in fluences of 1.5 and 0.5 mJ/cm^2, respectively. Hence the low-finesse A-FPSA is fully bleached by the pulse, whereas the high-finesse A-FPSA is only partially saturated (i.e., 30%), which reduces its effective modulation depth. At continuous-wave operation the saturable absorbers experience negligible bleaching.

Without dispersion compensation we obtained a pulse duration as short as 1.7 ps at 1.03 μm, using the high-finesse A-FPSA. The pulse repetition rate was 111 MHz, and the average output powers were typically 125–190 mW at an absorbed pump power of 1.2 W. The measured pulse widths agree within 1 order of magnitude with the pulse duration calculated from the fast saturable absorber model.[17,18] The model provides only an approximation because the dominant absorber response time for the 1.7-ps pulse is determined by the carrier lifetime of 3.8 ps, which is actually slightly longer than the final pulse duration. The time–bandwidth product is 0.6.

With dispersion compensation, using the high-finesse A-FPSA, we obtained subpicosecond pulses of 900-fs duration at a wavelength of 1.05 μm, a pulse repetition rate of 81 MHz, and output powers of 150 mW at 1-W absorbed pump power. Using the low-finesse A-FPSA, with the 30-nm thin absorber, we obtained solitonlike pulses of 570-fs FWHM at 1.05 μm, a pulse repetition rate of 75 MHz, and output powers of 170 mW at 900-mW absorbed pump power [Fig. 3(a)]. In both cases the time–bandwidth product of the pulses was typically 0.35, indicating close to transform-limited sech^2 pulse shape of a soliton. Because the 200-fs fast response time of the saturable absorber is shorter than the pulse duration obtained, both the fast saturable absorber[17,18] and the soliton mode-locking model[19,20] correctly predict the measured

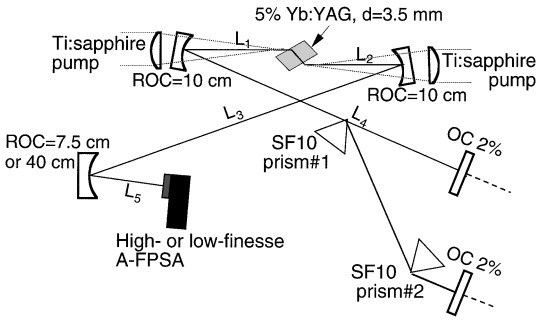

Fig. 2. Yb:YAG laser setup. $L_1 = L_2 = 5$ cm, $L_3 = 80$ cm, $L_4 = 40$ cm without and 90 cm with dispersion compensation (distance between the two SF10 prisms 75 cm), $L_5 = 3.9$ cm with the high-finesse A-FPSA and 20.5 cm with the low-finesse A-FPSA. OC's, output couplers.

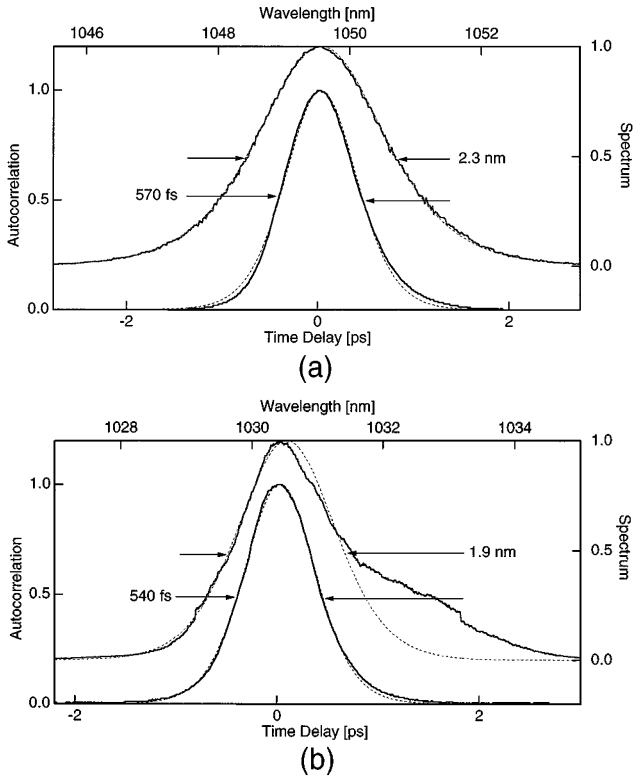

Fig. 3. Pulses obtained with dispersion compensation with the low-finesse A-FPSA designed for (a) 1.05 μm and (b) 1.03 μm. The dashed curves are fits to an ideal sech^2 pulse shape.

pulse durations. The high-finesse A-FPSA supports only longer pulses because at the available pump power we could only partially bleach the saturable absorber, resulting in a reduced modulation depth and therefore in an increased pulse duration.

We also designed two different low-finesse samples to obtain mode locking at either 1.03 or 1.05 μm. The emission cross section of Yb:YAG is approximately eight times larger at 1.03 μm (i.e., 2.3×10^{-20} cm^2) than at 1.05 μm (3×10^{-21} cm^2), but the absorption cross section is significantly higher at 1.03 μm (1.5×10^{-21} cm^2) than at 1.05 μm ($\approx 0.2 \times 10^{-21}$ cm^2).[21] Therefore we obtained mode locking at 1.05 μm with an absorber band gap designed for Nd:glass crystals that introduced a higher loss at 1.03 than at 1.05 μm. With the appropriate design of the low-finesse A-FPSA we also observed self-starting mode-locked pulses of 540-fs duration at 1.03 μm [Fig. 3(b)] with an average output power of 100 mW at 750-mW absorbed pump power. The pulse spectrum differs from the sech^2 shape because the Yb:YAG fluorescence spectrum at 1.03 μm deviates from a parabolic profile. The spectrum of the 540-fs pulse covered approximately one third of the bandwidth of the 1.03-μm emission line. An improved saturable absorber with a higher modulation depth should lead to more mode-locked bandwidth and shorter pulse generation.

In conclusion, we have demonstrated a Ti:sapphire-pumped passively mode-locked femtosecond Yb:YAG laser using two different design regimes of the A-FPSA, a low- and high-finesse A-FPSA. This result demonstrates the basic feasibility of femtosecond Yb:YAG lasers. The low-finesse A-FPSA was designed to maximize the modulation depth given the available power, which resulted in significantly shorter pulses. For future research we believe that the A-FPSA approach can be scaled along with the recently demonstrated power scalability of Yb:YAG lasers ultimately to yield a high-peak-power high-average-power femtosecond laser system.

The authors thank Franz Kärtner for helpful discussions, T. H. Chiu of AT&T Bell Laboratories for growing the high-finesse A-FPSA, and the Swiss priority program in optics for supporting this research.

References

1. P. Lacovara, H. K. Choi, C. A. Wang, R. L. Aggarwal, and T. Y. Fan, Opt. Lett. **16,** 1089 (1991).
2. T. Y. Fan, IEEE J. Quantum Electron. **29,** 1457 (1993).
3. A. Giesen, H. Hügel, A. Voss, K. Wittig, U. Brauch, and H. Opower, Appl. Phys. B **58,** 363 (1994).
4. U. Brauch, A. Giesen, M. Karszewski, C. Stewen, and A. Voss, Opt. Lett. **20,** 713 (1995).
5. R. Allen and L. Esterowitz, Electron. Lett. **31,** 639 (1995).
6. D. Kopf, F. X. Kärtner, K. J. Weingarten, and U. Keller, Opt. Lett. **20,** 1169 (1995).
7. D. Kopf, K. J. Weingarten, L. Brovelli, M. Kamp, and U. Keller, Opt. Lett. **19,** 2143 (1994).
8. D. Kopf, D. J. Weingarten, L. R. Brovelli, M. Kamp, and U. Keller, in *Conference on Lasers and Electro-Optics,* Vol. 15 of 1995 OSA Technical Digest Series (Optical Society of America, Washington, D.C., 1995), paper CWM2.
9. L. R. Brovelli, I. D. Jung, D. Kopf, M. Kamp, M. Moser, F. X. Kärner, and U. Keller, Electron. Lett. **31,** 287 (1995).
10. I. D. Jung, L. R. Brovelli, M. Kamp, U. Keller, and M. Moser, Opt. Lett. **20,** 1559 (1995).
11. U. Keller, D. A. B. Miller, D. G. Boyd, T. H. Chiu, J. F. Ferguson, and M. T. Asom, Opt. Lett. **17,** 505 (1992).
12. U. Keller, Appl. Phys. B **58,** 347 (1994).
13. L. R. Brovelli, U. Keller, and T. H. Chiu, J. Opt. Soc. Am. B **12,** 311 (1995).
14. S. R. Henion and P. A. Schulz, in *Conference on Lasers and Electro-Optics,* Vol. 12 of 1992 OSA Technical Digest Series (Optical Society of America, Washington, D.C., 1992), paper CThQ2, p. 540.
15. S. Tsuda, W. H. Knox, E. A. de Souza, W. Y. Jan, and J. E. Cunningham, Opt. Lett. **20,** 1406 (1995).
16. F. X. Kärtner, L. R. Brovelli, D. Kopf, M. Kamp, I. Calasso, and U. Keller, Opt. Eng. **34,** 2024 (1995).
17. H. A. Haus, J. Appl. Phys. **46,** 3049 (1975).
18. H. A. Haus, J. G. Fujimoto, and E. P. Ippen, J. Opt. Soc. Am. B **8,** 2068 (1991).
19. F. X. Kärtner and U. Keller, Opt. Lett. **20,** 16 (1995).
20. I. D. Jung, F. X. Kärtner, L. R. Brovelli, M. Kamp, and U. Keller, Opt. Lett. **20,** 1892 (1995).
21. D. S. Sumida, Hughes Research Laboratory, 3011 Malibu Canyon Road, Malibu, Calif. 90265, and T. Y. Fan, Lincoln Laboratory, Massachusetts Institute of Technology, Lexington, Mass. 02173 (personal communication).